Electrooxidation of some phenolic compounds at Bi-doped PbO$_2$

O. Shmychkova [a], T. Luk'yanenko [a], A. Yakubenko [b], R. Amadelli [c], A. Velichenko [a,*]

[a] Ukrainian State University of Chemical Technology, 8, Gagarin Ave., 49005 Dniepropetrovsk, Ukraine
[b] State Enterprise "Dnieprostandartmetrology", 23, Barykadna Str., 49044 Dniepropetrovsk, Ukraine
[c] Istituto per la Sintesi Organica e la Fotoreattivita – Consiglio Nazionale delle Recerche (ISOF-CNR), Dipartimento di Chimica, Universita di Ferrara, via L. Borsari, 46, 44121 Ferrara, Italy

ARTICLE INFO

ABSTRACT

It has been determined that bismuth content in the oxide grows from 0.49 to 1.81 wt% while increasing the Bi^{3+} ions additive concentration in the solution from 1 to 10 mM. It has been found that ionic additives affect the degree of hydroxylation of lead dioxide surface layer and the bond strength of the oxygen-containing particles. High surface hydration was observed for PbO$_2$ doped with Bi^{3+}. It was determined that the heterogeneous rate constant of oxidation of p-nitroaniline on modified lead dioxide ($k_v = 2.76 \times 10^{-2}$ min^{-1}) is half as much as on nonmodified ($k_v = 1.68 \times 10^{-2}$ min^{-1}). It has been revealed that the oxidation rate of p-nitrophenol and p-nitroaniline is proportional to the amount of hydroxyl radicals produced during the water oxidation, which is proposed to be used as a correlation parameter for predicting the electrocatalytic properties of materials based on lead dioxide in respect to the oxidation of organic compounds.

© 2014 Elsevier B.V. All rights reserved.

1. Introduction

The electrochemical oxidation of organic compounds is known to be a subject of scientific research during the past few years [1]. The oxidation of phenolic compounds has been of particular interest owing to their abundant presence in industrial wastewaters [1,2]. Such processes had been extensively studied with the main focus on type of anode material used [3,4].

Electrodes based on lead dioxide doped by ionic additives are known to be of great interest for investigation owing to tailoring solid state properties as well as electrocatalytic activity of PbO$_2$ [4–13]. Particular attention should be paid to ionic additives in high oxidation state +3 compared to places of cation vacancies of lead dioxide, in which Pb^{2+}-ions are known to be localized. It is recognized [14], that there are two zones on the lead dioxide surface: hydrated, where Pb^{2+} ions are associated with an appropriate amount of hydroxyl ions, and crystal, where Pb^{4+} ions in crystal lattice are octahedrally coordinated to O^{2-} ions. Lead ions replacement both in hydrated and crystal zone would cause not only the change of amount of oxygen-containing particles in each zone, but their binding energies, that in turn will change the electrocatalytic activity of materials.

In the present work we examine the electrocatalytic reactivity of PbO$_2$-anodes electrodeposited from methanesulfonate electrolytes that additionally contain Bi^{3+} ions in respect to processes with oxygen-containing particles participation, in particular to ozone evolution and oxidation of phenolic compounds. On the one hand, PbO$_2$-materials deposited from methanesulfonate electrolytes represent a considerable interest due to their high electrochemical stability and better mechanical properties in comparison with the same oxide, obtained from perchlorate, nitrate, acetate and alkaline solutions [15,16]. On the other hand, despite a large number of publications [1,2], several issues on Bi effects remain to be explained to draw definitive conclusions about correlation between type of deposit and its electrocatalytic reactivity.

2. Material and methods

All chemicals were reagent grade. Electrodeposition regularities of doped lead dioxide were studied on a Pt disk electrode (Pt-DE, 0.19 cm^2) in the methanesulfonate electrolytes that contained 1 M CH$_3$SO$_3$H, 0.01 M Pb(CH$_3$SO$_3$)$_2$ and 0.01 M Bi(NO$_3$)$_3$, by steady-state voltammetry. The Pt-DE surface was treated, before use, by the procedure described in [17]. Such preliminary treatment permits to achieve a reproducible surface. Voltammetry measurements were carried out in a standard temperature-controlled three-electrode cell. The platinum wire was the counter electrode. All potentials were recorded and reported vs. Ag/AgCl/KCl$_{(sat.)}$.
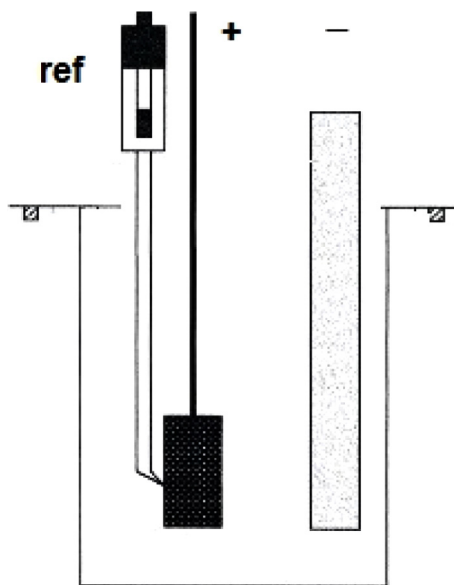
Scheme 1. Diagram of the electrochemical cell to study anodic oxidation of organics. +, PbO_2-anode; −, stainless steel cathode; ref, reference electrode.

Fig. 1. Current efficiency of PbO_2 versus potential of electrodeposition from 0.01 M $Pb(CH_3SO_3)_2 + 1$ M CH_3SO_3H (1); (1) + 0.01 M Bi^{3+} (2).

The determination of current efficiency and partial current of lead dioxide deposition was done by polarizing the electrode at a chosen potential above 1.4 V for 30 s÷5 min (depending on potential value) and measuring coulometrically the total charge passed during electrolysis. Subsequently, the charge passed for the cathodic reduction of the pre-formed PbO_2 was also measured coulometrically, in the background electrolyte, in the potential range from established potential to 0.9 V. As shown earlier [17], at slow sweep rates, quantitative reduction of PbO_2 takes place for thin oxide films. For relatively thick films, the adequacy of this method was confirmed by gravimetric experiments that show a direct proportionality between charge and amount of deposited PbO_2, as reported in the above cited publications. Then, in all cases, the data enable one to evaluate current efficiency for PbO_2 electrodeposition.

Platinized titanium was used as substrate. Titanium sheet was treated as described in [9] before platinum layer depositing. Lead dioxide coatings were electrodeposited at anodic current density 10 mA cm^{-2} and temperature (282 ± 2) K [10]. The coating thickness was ~50 μm. The determination of modifying additive in anodic materials was carried out photometrically with thiourea [18]. Solutions extinction was determined with blue light optical filter at 400 nm. It was established that lead dioxide modified by bismuth is formed when Bi^{3+} ions are present in the deposition electrolyte.

Lead dioxide anodes surface morphology was studied by scanning electron microscopy (SEM) with SEM-106I microscope.

XPS studies were carried out on a PHI 5000 spectrometer using monochromatic AlKα radiation for excitation. The BE value of C(1s), due to adventitious carbon and residual solvent, is 284.8($\pm$0.3) eV.

The electrooxidation of organic compounds was carried out in undivided cell at $j_a = 50$ mA cm^{-2} (Scheme 1). The volume of anolyte was 50 cm^3. Solution containing phosphate buffer (0.25 M $Na_2HPO_4 + 0.1$ M KH_2PO_4) + 2×10^{-4} M organic compound (pH = 6.55), was used as electrolyte. Stainless steel was used as cathode. Lead dioxide electrodes modified by bismuth were used as anodes. Electrode surface area was 1 cm^2.

Analyses of the reaction products were conducted by HPLC using a Shimadzu RF-10A xL instrument equipped with a Ultraviolet SPD-20AV detector and a 30 cm Discovery® C18 column. Ozone analysis was carried out mostly by iodometric titration [19]. In some cases
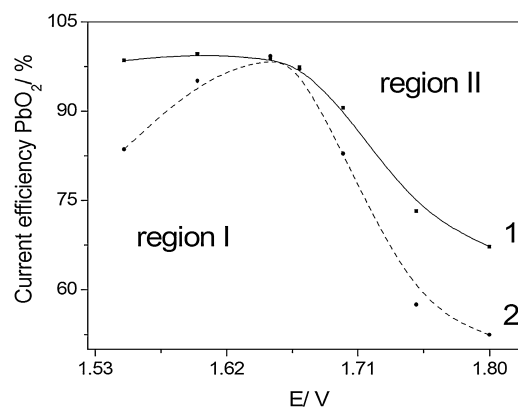
the results were checked by the spectrophotometric method. The formation of colored compounds during electrolysis was followed by UV–visible spectroscopy using a Kontron Uvikon 940 spectrometer.

There are some methods for detection of reactive oxygen species [20,21]. In order to measure the hydroxyl radicals (OH•) dissolved in the liquid, we used the fluorescence method based on terephthalic acid (TA) [22,23]. Terephthalic acid is a well known OH scavenger that can be used for estimation of the relative amount of OH radicals generated under various conditions. The OH radical can convert terephthalic acid to 2-hydroxyterephthalic acid (HTA). When the solution containing TA and HTA molecules is irradiated by UV light, HTA molecules emit light at $\lambda = 313$ nm, while TA molecules do not. Moreover, terephthalic acid does not react directly with other radicals, such as superoxide anion, organic hydroperoxide, with formation of HTA [22,23]. As TA has a symmetrical structure, there is only one form of monohydroxylated adduct. Saran and Summer [24] discussed other properties of TA making it highly sensitive marker toward OH-radicals. Fluorescence spectra were recorded in the wavelength range 350–550 nm at $\lambda_{exit} = 313$ nm using a FluoroMax fluorometer 2 (ISA Jobin Yvon Spex Instruments SA Inc.).

3. Results and discussion

3.1. Regularities of lead dioxide electrodeposition from methanesulfonate electrolytes

Since the formation of lead dioxide takes place simultaneously with the oxygen evolution reaction we investigated the current efficiency of PbO_2 depending on the electrodeposition potential (Fig. 1).

At low polarizations (region I) PbO_2 current efficiency remains constant, close to 100% (in the electrolyte without Bi^{3+}) or increases with the current density growth, scaling up to 100% in the case of a significant inhibition of Pb^{2+} ions oxidation by adsorption of ionic additive (Bi^{3+}) [10], which exhibits its own electrochemical activity. In this region, the deposition process is kinetically controlled. In region II, the current efficiency reduces due to increase of the rate of oxygen evolution reaction at a limiting current of an oxide electrodeposition (diffusion control).

It has been shown [7,16,17,25] that some amounts of foreign ions, surfactants, polyelectrolytes and oxides as additives to the deposition electrolyte cause changes in electrodeposition kinetics, physico-chemical properties of resulting oxides and their electrocatalytic activity. Unfortunately, no information about the content of dopant is stated in the most of papers that does not allow obtaining oxides with a given composition by direct electrochemical

Table 1
Bismuth content in lead dioxide coatings depending on nature of deposition electrolyte.

Solution	Dopant content (wt%)
$0.1\,M\,Pb(CH_3SO_3)_2 + 1\,M\,CH_3SO_3H + 0.0004\,M\,Bi^{3+}$	0.24
$0.1\,M\,Pb(CH_3SO_3)_2 + 1\,M\,CH_3SO_3H + 0.0008\,M\,Bi^{3+}$	0.36
$0.1\,M\,Pb(CH_3SO_3)_2 + 1\,M\,CH_3SO_3H + 0.001\,M\,Bi^{3+}$	0.49
$0.1\,M\,Pb(CH_3SO_3)_2 + 1\,M\,CH_3SO_3H + 0.01\,M\,Bi^{3+}$	1.81

synthesis. Most likely, as in the case of metallic deposits, the content of dopant in the oxide will depend on its concentration in the electrolyte.

Since Bi^{3+} ions can absorb on the oxide electrodes surface [16,17,26], they, probably, can in certain amounts incorporate in materials involved. Herewith bismuth content in the oxide grows from 0.49 to 1.81 wt% while increasing the Bi^{3+} ions additive concentration in the solution from 1 to 10 mM (Table 1).

3.2. Chemical composition of coatings

SEM/EDAX experiments were performed to evaluate the amount and distribution of dopants in electrodeposited PbO_2. Analysis of different portion of the sample showed that bismuth is well distributed within the deposit with an amount of ~2% (Appendix A). This value is confirmed by photometry measurements after chemical dissolution of the PbO_2 layer. At the same time, the average O/Pb ratio was 2.15 and 3.3 ± 0.01 in the absence and in the presence of Bi, respectively [10].

To get further insight into the effects of doping, we investigated the surface layers by X-ray photoelectron spectroscopy. The XPS spectra have been discussed in detail in our recent publications [10–12].

Previous works on the XPS characterization of PbO_2 [27] pointed out the importance of the examination of O1s region as it provides information on the hydration state of the surface. In particular Ni causes a very high accumulation of oxygen with respect to PbO_2 stoichiometry [27].

In the present work, collected spectra show two peaks: the one at the lower binding energy was assigned to strongly bounded lattice oxygen, while the broader one at higher binding energy was attributed to weakly bound oxygen species: adsorbed OH^- and water [27], that means interaction with water in outer regions (Fig. 2a). Ionic additive affect the degree of hydroxylation of lead dioxide surface layer and the bond strength of the oxygen-containing particles. The high surface hydration was determined for oxides doped with Bi^{3+} (Fig. 2b). Observed effect is due to introduction of ionic additive both at cation vacancies places and in the crystal lattice.

3.3. Electrocatalytical properties of materials

Such changes in the surface concentration of oxygen-containing particles adsorbed on the electrode will also influence the electrocatalytic activity of anodes that depends on chemical (composition of material) and geometrical factors such as morphology and structure [28]. So the next step of our work was to evaluate the electrocatalytic activity of materials in relation with so-called oxygen-transfer processes that occur through the initial stage of the formation of oxygen-containing particles of radical type adsorbed on the electrode surface.

It is now well recognized that, in the direct electrolysis process, the oxidation of a large number of organic and inorganic compounds on different electrode materials, including PbO_2, proceeds simultaneously with the evolution of oxygen. Highly oxidizing oxygen species, such as OH radicals, formed during the anodic
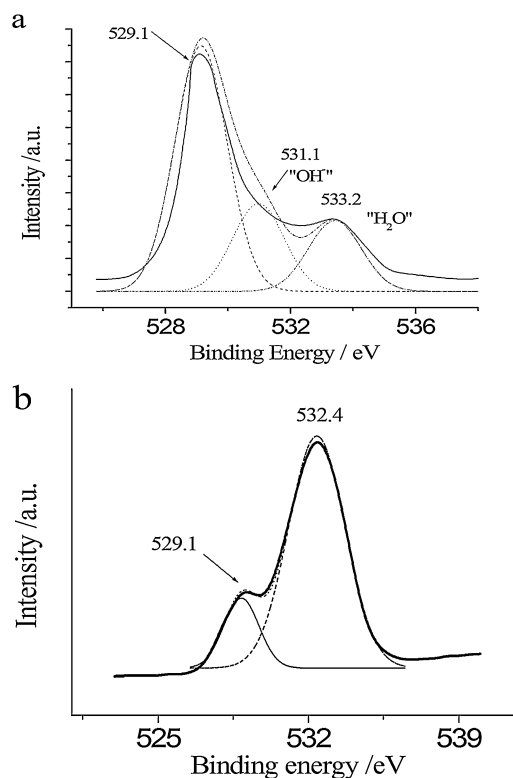

Fig. 2. O 1s core level structures in PbO_2 (a) PbO_2-1.81 wt% Bi (b) obtained at $j_a = 10\,mA\,cm^{-2}$.

oxidation of water are able, in turn, to oxidize most of organic compounds. There is a vast literature on this subject, concerning PbO_2-anodes [15,25,29–31].

According to obtained results (Fig. 3), an activity of PbO_2-1.81 wt% Bi coating toward generation of hydroxyl radicals is sensibly higher than that of nonmodified deposit. In connection with such significant alterations in the activity of coatings toward the generation of hydroxyl radicals the comparison of data considering an average amount of OH radicals and the electrocatalytical activity of coatings involved toward the oxidation of organic compounds is seemed to be of considerable interest. This fact will be commented later in this section.

Since ozone generation occurs simultaneously with processes of organic compounds oxidation [15], its synthesis during the electrolysis would facilitate the destruction of toxic organic substances. In this connection, we carried out some experiments under conditions in which formation and detection of O_3 is improved [32], i.e.,
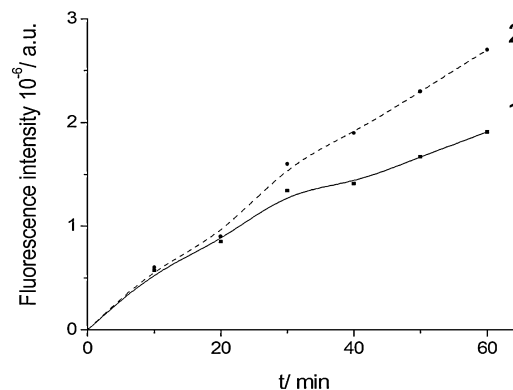

Fig. 3. Fluorescence intensity of 2-hydroxyterephthalate during electrolysis on PbO_2 (1) and PbO_2-Bi (2) at $j_a = 50\,mA\,cm^{-2}$.

in buffer phosphate electrolyte at low temperature after a short anodic pretreatment of the electrode at higher current density that allows increasing of the current efficiency of ozone at low current densities. Current efficiencies for ozone formation at a current of 50 mA cm^{-2} were 0.29 and 0.96% for undoped PbO$_2$ and doped by Bi^{3+} PbO$_2$, respectively.

According to the obtained results, one can conclude that ozone current efficiencies on electrodes synthesized from methanesul-fonate bath are three times lower than on deposits obtained from nitrate bath [15]. Doping slightly increases the current efficiency of ozone, but the latter is characterized by values in a range of several percent.

We think that such an effect is due to alterations in the chemical composition of deposits obtained from nitrate and methanesul-fonate baths, in particular due to alterations in the degree of surface hydroxylation. Since it is believed that oxygen-containing species strongly bonded to the surface take part in the reaction of ozone evolution [15], decrease of their amount would lead to drop in ozone current efficiency that one can observe in the case of coatings, obtained from methanesulfonate electrolytes.

We chose aromatic compounds, namely 4-nitroaniline and 4-nitrophenol for elucidation of the nature of electrocatalytic activity of anode materials based on lead dioxide toward the oxidation of organic compounds. Such choice was due to the fact that processes of electrochemical oxidation of phenolic compounds at the different electrodes are quite well understood, so the view can be focused only on clarifying the role of anode material.

Phenol and its derivatives are considered to be the most common highly toxic persistent organic pollutants. Among them nitro-aromatics are widely used as synthetic intermediates in pharmaceutical, dyes, pesticide industry [21]. There is a vast literature on this subject, in which IrO$_2$ and other noble metals oxides, PbO$_2$ or SnO$_2$ were used as anode materials for removal of these pollutants from wastewaters [4,15,17,25,31]. Acidity of electrolysis solution is important choice, because it affects the processes of acids and bases dissociation, as well as individual steps of such reactions. Anodic oxidation of phenols, for example, may undergo two possible oxidation pathways, depending on the acid–base properties of the system [29,33]. It should be pointed out that the most of oxide materials are chemically and corrosion resistant only in alkaline solutions. Noble metal oxides, lead, tin and manganese dioxides are just ones stable in neutral and acidic solutions. Electrocatalytic activity of the noble metal oxides for direct anodic oxidation of phenolic compounds is rather low, whereas lead dioxide in these processes exhibit relatively high activity [1–5,15,29].

3.3.1. p-Nitroaniline oxidation

As shown in [1], the overall mechanism for the electrochemical oxidation of phenols involves three consecutive irreversible steps: (i) oxidation of the phenolic compound to a quinoid compound; (ii) ring opening reaction with formation of aliphatic acids; (iii) mineralization to CO$_2$. According to literature data [34], relatively large number of intermediates is formed during the anodic oxidation of p-nitroaniline. Main intermediates are benzoquinone and maleic acid. We conducted analyses of the reaction products by HPLC to determine the possibility of using the proposed mechanism. It was established that 1,4-benzoquinone is one of intermediate products (Fig. 4). Upon the prolonged electrolysis it is possible to determine only aliphatic acids. Time of disappearance of aromatic intermediates and the change in concentration of the initial compound were determined from electronic absorption spectra of solutions at various time of electrolysis. The initial solution features by peaks at 230 and 380 nm that correspond to the presence of a chromophore group in the compound (Appendix B). During the electrolysis the intensity of a peak at $\lambda = 380$ nm decreases and after some hours the solution stops to absorb in visible spectrum. However there is an
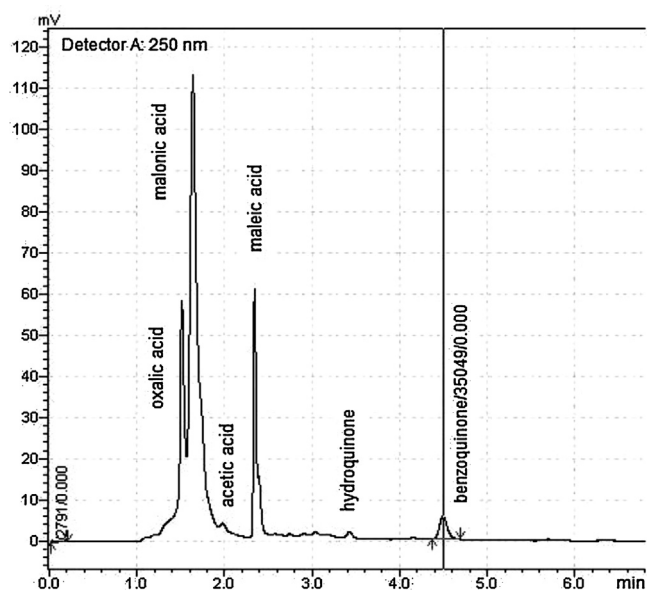

Fig. 4. Chromatogram of p-nitroaniline solution (2 mM) after 14 h of electrolysis at $j_a = 50$ mA cm^{-2}.

absorbance in the ultraviolet region still that indicates an aromatic structure in the intermediate formed.

Plot of electrolysis time versus a natural logarithm of the concentration of the initial compound indicates the pseudo-first order with respect to p-nitroaniline (Fig. 5). As chromatography and UV spectroscopy revealed the same products as in the mechanism proposed by Anotai et al. [35], we suggest that the investigated reaction proceeds in accordance with this mechanism, where benzoquinone is the main intermediate product. Since the electrochemical destruction of p-nitroaniline proceeds through the benzoquinone formation stage, we have investigated the electrochemical oxidation of latter compound. The initial spectrum of benzoquinone features by peak at $\lambda = 240$–250 nm in UV region (Appendix C). During the electrolysis absorption intensity decreases, the plateau appears at 270–310 nm, indicating the formation of aromatic intermediates.

According to kinetic curve data, one can conclude that the electrooxidation of benzoquinone is also a pseudo-first order reaction. The heterogeneous rate constant of oxidation of benzoquinone ($k_v = 4.2 \times 10^{-2}$ min^{-1}) is higher, than for p-nitroaniline ($k_v = 1.68 \times 10^{-2}$ min^{-1}). Obtained data are in good agreement with literature data and do not contradict the mechanism presented in [35].
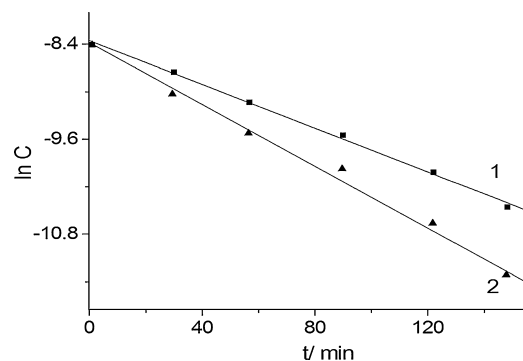

Fig. 5. Plot of electrolysis time versus a natural logarithm of the concentration of the initial compound on PbO$_2$ (1) and PbO$_2$-Bi (2)-anodes.
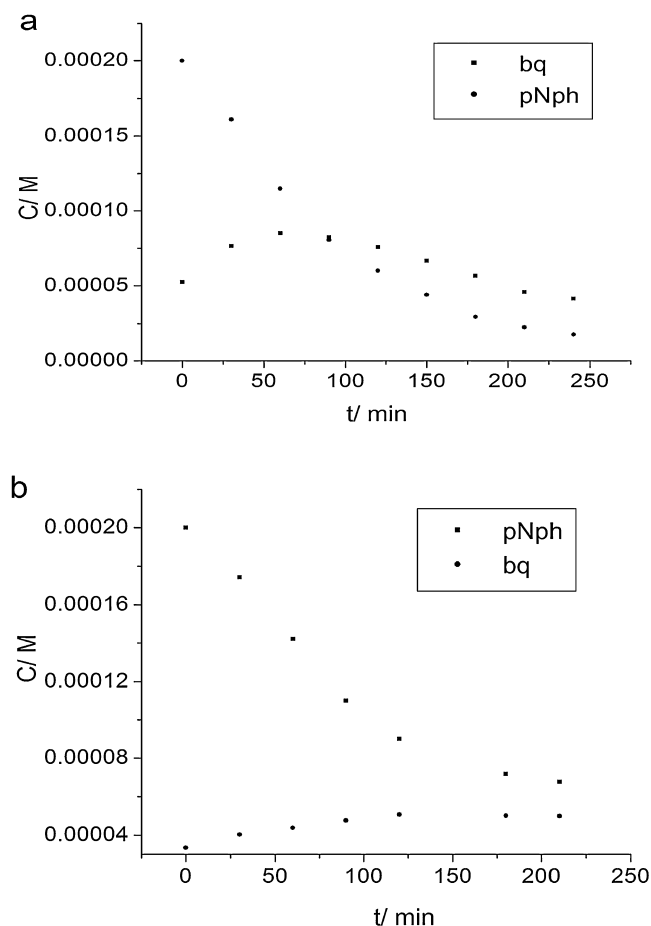
Fig. 6. Change of concentration of p-nitrophenol (pNph) and benzoquinone (bq) solutions during electrolysis in carbonate buffer (a) and acidic medium (b).

It should be pointed out that processes of p-nitroaniline electrooxidation on modified and nonmodified PbO_2 are qualitatively similar and differ only in rate. This suggests the constancy of mechanism of oxidation and allows one to carry out a correct comparison of their electrocatalytic reactivity. It was determined that the heterogeneous rate constant of oxidation of p-nitroaniline on modified lead dioxide ($k_v = 2.76 \times 10^{-2}$ min^{-1}) is half as much as on nonmodified ($k_v = 1.68 \times 10^{-2}$ min^{-1}, see Fig. 5).

3.3.2. p-Nitrophenol oxidation

p-Nitrophenol is known to be dissociated in the solution. In the acid medium where the concentration of hydrogen ions is high, the compound exists in ionic form. According to the chromophore theory, the molecular structure of the p-nitrophenol varies according to benzenoid–quinoid tautomerism with pH changing. p-Nitrophenol is strongly associated due to the formation of hydrogen bonds between the hydroxyl and nitro groups [21]. We carried out experiments both in the alkaline, acidic media and phosphate buffer to study the reactivity of p-nitrophenol in respect with the electrochemical oxidation (Appendix D).

In carbonate solutions, the rate of destruction of the initial compound has been significantly increased. The fast conversion in this case was accompanied by the appearance of intense brown coloration due to the appearance of stable intermediates, but a further increase of electrolysis time resulted in a rapid disappearance of the solution color. It should be pointed out that at 50% conversion of the initial p-nitrophenol, the concentration of p-benzoquinone, produced during the reaction is maximal and it is a half of the initial concentration of organic compound (Fig. 6a), that was not observed during the electrolysis in an acidic medium (Fig. 6b). Oxidation of 2 mM p-nitrophenol occurs almost entirely in 18 h of electrolysis at 50 mA cm^{-2}. Thus, as the electrolysis products maleic acid and stoichiometric amount of NO_3^- were detected by HPLC. 1,4-Benzoquinone was also one of aromatic intermediate products, but its concentration was single-order higher than during the oxidation of p-nitroaniline (Fig. 7). The latter indicates a more effective destruction of the aromatic ring in the case of p-nitroaniline.
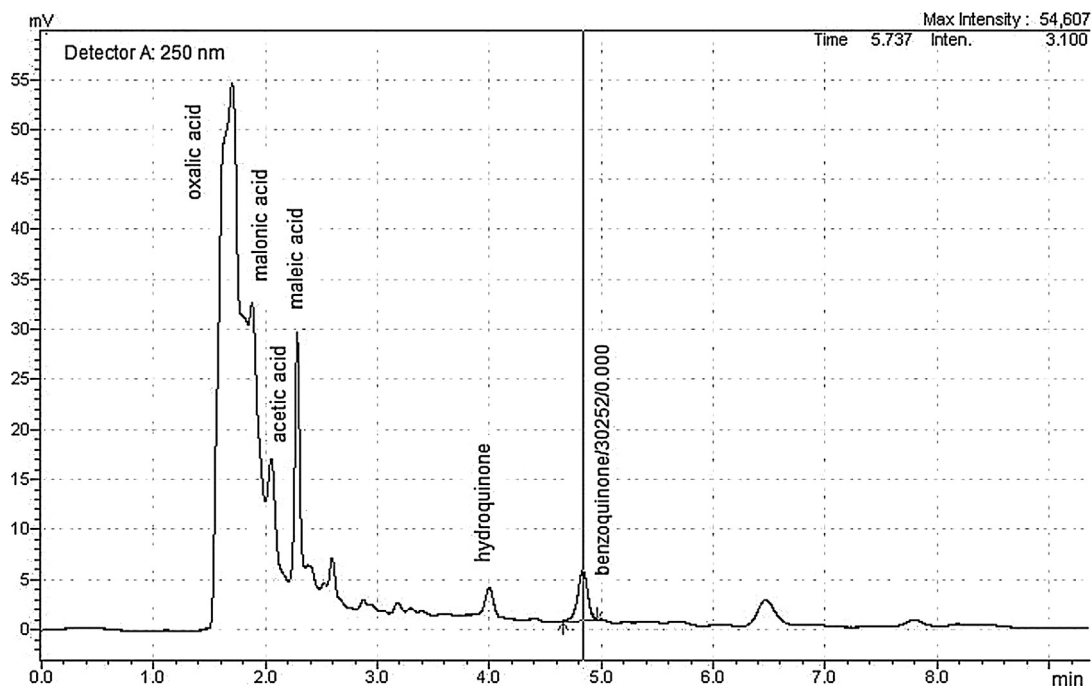

Fig. 7. Chromatogram of p-nitrophenol solution (2 mM) after 14 h of electrolysis at j_a = 50 mA cm^{-2}.

The rate constants for p-nitrophenol oxidation on modified lead dioxide electrodes are somewhat lower than those for p-nitroaniline but a modified by bismuth PbO_2 also exhibits a higher electrocatalytic activity.

According to obtained results one can conclude that the oxidation rate of p-nitrophenol and p-nitroaniline is proportional to the amount of oxygen-containing radicals (hydroxyl radicals) produced during the water oxidation (see Fig. 3), which is proposed to be used as a correlation parameter for predicting the electrocatalytic properties of materials based on lead dioxide in respect to the oxidation of organic compounds.

4. Conclusions

The bismuth content in the oxide grows from 0.49 to 1.81 wt% while increasing of Bi^{3+} ions additive concentration in the solution from 1 to 10 mM. Ionic additives affect the degree of hydroxylation of lead dioxide surface layer and the bond strength of the oxygen-containing particles. High surface hydration was observed for PbO_2 doped with Bi^{3+}.

The oxidation rate of p-nitrophenol and p-nitroaniline is proportional to the amount of oxygen-containing radicals produced during the water oxidation, which is proposed to be used as a correlation parameter for predicting the electrocatalytic properties of materials based on lead dioxide in respect to the oxidation of organic compounds.

Electrocatalysts based on PbO_2, doped with Bi^{3+} ions may be recommended as anodes for the electrochemical conversion of p-nitrophenol and p-nitroaniline, and other toxic organic substances.

Appendix A. Supplementary data

Supplementary data associated with this article can be found, in the online version, at http://dx.doi.org/10.1016/j.apcatb.2014.07.011.

References

[1] C. Borras, T. Laredo, J. Mostany, B.R. Scharifker, Electrochim. Acta 49 (2004) 641–648.
[2] C. Borras, T. Laredo, B.R. Scharifker, Electrochim. Acta 48 (2003) 2775–2780.
[3] Y. Cong, Z. Wu, J. Phys. Chem. C 111 (2007) 3442–3446.
[4] Y. Liu, H. Liu, Electrochim. Acta 53 (2008) 5077–5083.
[5] X. Li, D. Pletcher, F.C. Walsh, Chem. Soc. Rev. 40 (2011) 3879–3894.
[6] A.B. Velichenko, R. Amadelli, A. Benedetti, D.V. Girenko, S.V. Kovalyov, F.I. Danilov, J. Electrochem. Soc. 149 (2002) C445–C449.
[7] A.B. Velichenko, D. Devilliers, J. Fluorine Chem. 128 (2007) 269–276.
[8] C.T.J. Low, D. Pletcher, F.C. Walsh, Electrochem. Commun. 11 (2009) 1301–1304.
[9] O. Shmychkova, A. Magamedova, D. Girenko, T. Luk'yanenko, A. Velichenko, Chem. Chem. Technol. 7 (2013) 365–368.
[10] O. Shmychkova, T. Luk'yanenko, A. Velichenko, L. Meda, R. Amadelli, Electrochim. Acta 111 (2013) 332–338.
[11] O. Shmychkova, T. Luk'yanenko, A. Velichenko, R. Amadelli, J. Electroanal. Chem. 706 (2013) 86–92.
[12] O. Shmychkova, T. Luk'yanenko, R. Amadelli, A. Velichenko, J. Electroanal. Chem. 717–718 (2014) 196–201.
[13] O.B. Shmychkova, T.V. Luk'yanenko, L.V. Dmitrikova, A.B. Velichenko, Prot. Met. Phys. Chem. Surf. 50 (2014) 218–222.
[14] P. Ruetschi, R. Giovanoli, Power Sources 13 (1991) 81–97.
[15] R. Amadelli, L. Samiolo, A. De Battisti, A.B. Velichenko, J. Electrochem. Soc. 158 (2011) P87–P92.
[16] S.E. Treimer, J. Feng, D.C. Johnson, J. Electrochem. Soc. 148 (2001) E321–E325.
[17] A.B. Velichenko, D.V. Girenko, S.V. Kovalyov, A.N. Gnatenko, R. Amadelli, F.I. Danilov, J. Electroanal. Chem. 454 (1998) 203–208.
[18] Z.S. Mukhina, E.I. Nikitina, L.M. Budanova, R.S. Volodarskaya, L.Y. Polyak, A.A. Tikhonova, Methods of Analysis of Metals and Alloys (in Russian), State Publishing House of Defense Industry, Moscow, 1959.
[19] Y.M. Vera, R.J. de Carralho, M.L. Torem, B.A. Calfa, Chem. Eng. J. (Amst., Neth.) 155 (2009) 691–697.
[20] E. Mahe, P. Bornoz, E. Briot, J. Chevalel, C. Comninellis, D. Devilliers, Electrochim. Acta 102 (2013) 259–273.
[21] S. Reyna, J.L. Sanchez, E.R. Bandala, J.M. Peralta-Hernandez, C.A. Martinez-Huitle, M.A. Quiroz, Sustain. Environ. Res. 21 (2011) 321–328.
[22] N. Soh, Anal. Bioanal. Chem. 386 (2006) 532–543.
[23] K.R. Millington, L.J. Kirschenbaum, Color. Technol. 118 (2002) 6–14.
[24] M. Saran, K.H. Summer, Free Radic. Res. 31 (1999) 429–436.
[25] Y. Liu, H. Liu, J. Ma, Appl. Catal. B 91 (2009) 284–299.
[26] R. Amadelli, A. De Battisti, D.V. Girenko, S.V. Kovalyov, A.B. Velichenko, Electrochim. Acta 46 (2000) 341–347.
[27] R. Amadelli, L. Armelao, E. Tondello, S. Daolio, M. Fabrizio, C. Pagura, A. Velichenko, Appl. Surf. Sci. 142 (1999) 200–203.
[28] S. Trasatti, Electrochim. Acta 45 (2000) 2377–2385.
[29] M.A. Quiroz, S. Reyna, C.A. Martinez-Huitle, S. Ferro, A. De Battisti, Appl. Catal. B 59 (2005) 259–266.
[30] J. Iniesta, J. Gonzalez-Garcia, E. Exposito, V. Montiel, A. Aldaz, Water Res. 35 (2001) 3291–3300.
[31] J. Kim, G.V. Korshin, A.B. Velichenko, Water Res. 39 (2005) 2527–2534.
[32] P.C. Foller, G.H. Kelsall, J. Appl. Electrochem. 23 (1993) 996–1010.
[33] H. Liu, Y. Liu, C. Zhang, R. Shen, J. Appl. Electrochem. 38 (2008) 101–108.
[34] J. Widera, J.A. Cox, Electrochem. Commun. 11 (2002) 8–12, 2.
[35] J. Anotai, M.-C. Lu, P. Chewpreecha, Water Res. 40 (2006) 1841–1847.